Left-Right Brain-Wide Asymmetry of Neuroanatomy in the Mouse Brain.

Andrew Silberfeld[1,2], James M. Roe[3], Jacob Ellegood[4,5], Jason P. Lerch[5,6,7,8], Lily Qiu[5,7], Yongsoo Kim[9], Jong Gwan Lee[1,2], William D. Hopkins[10], Joanes Grandjean[11,12], Yangming Ou[13], Olivier Pourquié[1,2].

Affiliations:

1. Department of Genetics, Harvard Medical School, Boston, MA, USA.
2. Department of Pathology, Brigham and Women's Hospital, Boston, MA, USA.
3. Center for Lifespan Changes in Brain and Cognition (LCBC), Department of Psychology, University of Oslo, Norway.
4. Bloorview Research Institute, Holland Bloorview Kids Rehabilitation Hospital, Toronto, Ontario, Canada.
5. Mouse Imaging Centre, Hospital for Sick Children, Toronto, Ontario, Canada.
6. Department of Medical Biophysics, The University of Toronto, Toronto, ON, Canada.
7. Department of Neurosciences and Mental Health, The Hospital for Sick Children, Toronto, ON, Canada.
8. Department of Preclinical Imaging, Wellcome Centre for Integrative Neuroimaging, University of Oxford, Oxford, UK.
9. Department of Neural and Behavioral Sciences, College of Medicine, The Pennsylvania State University, Hershey, PA, USA.
10. Department of Comparative Medicine & Michale E Keeling Center for Comparative Medicine and Research, The university of Texas MD Anderson Cancer Center.
11. Donders Institute for Brain, Behaviour, and Cognition, Nijmegen, Netherlands.
12. Department for Medical Imaging, Radboud University Medical Center, PO Box 9101, Nijmegen, Netherlands.
13. Boston Children's Hospital, Harvard Medical School, Harvard University, Boston, MA, USA.

Corresponding Author:

Dr. Olivier Pourquié

Email: pourquie@genetics.med.harvard.edu

Author Contributions: A.S. and O.P. designed all experiments and wrote the paper. A.S. performed all experiments, data analysis and computer programming related to mice and non-human primates. J.M.R. performed all FreeSurfer analysis with human subjects. A.S. analyzed human FreeSurfer cohort summaries. J.E. and J.P.L. provided MRI scans from Qiu et al. 2018. J.E., J.P.L. and L.Q. contributed information critical for determining left-right orientation for the POND and Qiu et al. 2018 cohorts. Y.K. provided left-right orientation information for the BICCN and Newmaster et al. 2020 cohorts. W.D.H. provided the Chimpanzee MRI scans along with left-right orientation information. J.G.L and J.G. helped with interpretation of the data. Y.O. helped with interpretation of the data and provided critical input and feedback for study design. All authors contributed to the editing of the manuscript.

Competing Interest Statement: The authors have no competing interests to

disclose.

Abstract

Left-right asymmetry of the human brain is widespread through its anatomy and function. However, limited microscopic understanding of it exists, particularly for anatomical asymmetry where there are few well-established animal models. In humans, most of the brain shows subtle, population-average, regional asymmetries in cortical thickness or surface area. In addition, a macro-scale twisting called the cerebral petalia exists in which the right hemisphere protrudes anteriorly relative to the left. Here, we ask whether neuroanatomical asymmetries can be observed in mice, leveraging 6 different neuroimaging cohorts of animals from 5 different research groups (~3,500 animals in total). We found an anterior-posterior pattern of volume asymmetry in mice, where anterior regions are larger on the right while posterior regions are larger on the left. This pattern appears driven by a similar trend in surface area asymmetry and is supported by a concordant pattern of positional asymmetries. The cerebral hemisphere as a whole appears shifted anteriorly on the right while the brainstem and cerebellum appear shifted anteriorly on the left. These results together indicate a small torsion of the brain is present in mice, similar to the cerebral petalia in humans. By establishing a signature of anatomical brain asymmetry in mice, we aim to provide a foundation for future studies to probe the mechanistic underpinnings of anatomical brain asymmetry seen in humans – a feature of the brain with extremely limited understanding.

Main Text

Introduction

A central feature of the vertebrate body plan is its bilaterally symmetrical left-right organization. Some structures, such as the visceral organs break this symmetry as a result of asymmetrical signaling during development[1]. The human brain appears generally symmetrical between sides but is nevertheless organized asymmetrically through its anatomy and function. Numerous cognitive abilities such as language and face recognition depend on circuitry that reliably exhibits greater activation on one side of the brain than the other, and does so in a consistent direction across the population[2–8]. Anatomically, most regions of the human brain show small population-average asymmetries of cortical thickness (CT) or surface area (SA)[9–12], in addition to a macro-scale "twisting" of the brain known as the *cerebral petalia* in which the right hemisphere is shifted anteriorly compared to the left[13–17]. Anatomical asymmetry of the posterior temporal lobe (the *planum temporale*) has been linked to functional asymmetry of human language, however studies show this relationship to be complex at the individual level[18–21].

Extensive research in humans on anatomical brain asymmetry has identified highly reproducible sets of CT and SA asymmetries[9,22] as well as an anterior-posterior pattern of CT asymmetry[9,22–24]. Neurodevelopmental and cytoskeletal genes associate with modified anatomical asymmetry[25] – with some of these genes also discovered in a recent handedness genome-wide association study[26]. Yet fundamental aspects of human anatomical brain asymmetry – especially those at the microscopic level – remain poorly understood and challenging to address in human subjects. For example, the mechanism by which asymmetries emerge is completely unknown. Some anatomical asymmetries are apparent *in utero* and persist into adulthood[11,27,28], suggesting that they are developmentally encoded. Yet, individuals with reversed visceral organ asymmetry generally do not show a reversed pattern of anatomical[29–32] or functional[29,33,34] brain asymmetries, suggesting largely distinct pathways between asymmetry-breaking of the brain and the internal organs. Other unanswered, fundamental questions include the cellular basis of anatomical asymmetry, the relationship between structural and functional asymmetry in the general population, and the mechanism behind the small shifts observed in anatomical and functional asymmetry among individuals with autism spectrum disorder[35,36] and schizophrenia[37,38].

Understanding of these questions would benefit substantially from animal models for conducting cellular-level studies of anatomical brain asymmetry. However, existing animal models have limitations which largely constrain their potential to inform understanding of human anatomical brain asymmetry. In zebrafish and *Drosophila*, well-defined asymmetries respectively exist in the habenula[39–41] and brainstem[42,43], but the rest of the brain in these animals shows no other apparent morphological asymmetries. This raises an important question about whether these isolated examples seen in distant species are fundamentally distinct from the extensive, subtle pattern of asymmetries seen brain-wide in humans. For example, the zebrafish habenula asymmetry is regulated by the nodal left-right pathway governing visceral organ asymmetry[40], while in humans, this pathway seems generally decoupled from brain asymmetries[29–34].

In non-human primates such as chimpanzees and macaques, asymmetry has been generally reported across many brain regions, but studies show limited reproducibility[44–50]. This is further complicated by the difficulty of comparing studies using different metrics (volume[44,45], SA[24], CT[24,51]), and different levels of granularity (voxel-based[50,51] vs atlas-based[24,49] results). One exception to this reproducibility challenge is the *planum temporale*, which is widely seen to be expanded in the left hemisphere in chimpanzees[24,44,52–55] and baboons[56–58] – similar to humans[59,60]. Yet, this represents the only well-defined example of asymmetry within those species. As a result,

humans remain the only species with a reliable and agreed-upon pattern of brain-wide anatomical asymmetry.

Alternatively, mice, which are a commonly used species for understanding the human brain's organization[61], are an ideal model organism for studying neuroanatomical asymmetry. Despite its overall appearance of symmetry, the mouse brain possesses many well-described functional asymmetries: processing of vocalizations and pitch sweeps[62–65], visceral stimuli[66], spatial memory[67–70], fear[71–74], and handedness[75]. In addition, numerous brain-wide structural imaging datasets and sensitive tools for morphometry analysis exist[76–79], allowing for investigation into neuroanatomical asymmetries along with replication analyses between cohorts – something that is largely absent from the existing non-human literature.

Two prior studies have investigated neuroanatomical asymmetry in mice using single cohorts, but as in primates, they reached conflicting descriptions. One study by Spring et al. 2010[80] showed an overall larger left hemisphere volume of 2.8% while a more recent study by Elkind et al. 2023[81] identified an asymmetry pattern varying regionally without any clear trend. The widespread availability of distinct imaging datasets from separate groups now provides the opportunity to comprehensively investigate this question in mice while accounting for the overall generalizability of the results.

Here, we investigate neuroanatomical asymmetry in mice using multiple cohorts from different imaging modalities. We found that anatomical brain asymmetry is indeed present in the adult mouse brain but is initially obscured by strong cohort-specific patterns of asymmetry without obvious trends. By instead looking for what is consistent between these groups of animals, we identified an anterior-posterior pattern of volume asymmetry where anterior regions are larger on the right and posterior regions are larger on the left. Yet, instead of appearing as distinct regional asymmetries such as in humans, the data overall indicates a small "twisting" of the brain in mice, similar to the cerebral petalia in humans. We thus propose mice as a novel mammalian animal model for investigating neuroanatomical asymmetry at the microscopic level. Future understanding of the genetic and cellular underpinnings of this asymmetry signature may provide insight into observations seen in humans.

Results

Pipeline Overview. To investigate anatomical asymmetry in the mouse brain, we performed automated image registration and morphometry analysis (**Fig. 1A**). Brain-wide imaging data was obtained from six different published studies performed by five different research groups. These studies used mice of different genetic backgrounds, with drastically varying numbers of animals (n = 23 to 2,992). We used three high-resolution serial histology studies (Serial Two-Photon Tomography; STPT) and three magnetic resonance imaging (MRI) studies (**Table S1**). We performed automated linear and non-linear image registration using the software package ANTsPy[78] to align each sample image to a symmetrical, three-dimensional (3D) reference template. This procedure outputs a 3D image (Jacobian determinant field) in which each pixel represents the local volumetric change between the original sample and the reference template. Using the pixel-wise annotations of the reference template (Common Coordinate Framework version 3; CCFv3), we integrated over this field and obtained region-specific measurements of volume for each hemisphere, from which we calculated left-right asymmetries. Animals of a single study are referred to here as a "cohort".

Reproducible Volume Asymmetries Exist Across Independent Cohorts. We found a large number of significantly asymmetric brain regions in each of the 4 largest cohorts as well as a substantial enrichment for significant asymmetries in the 2 smallest (**Fig. S1**). However, correlating these region-wise patterns across cohorts resulted in weak consistency between them (**Fig. 1B)**.

In contrast, sub-sampling 20 animals from a given cohort showed much stronger consistency within-cohorts (**Fig. 1C**). Thus, these asymmetry patterns, despite their significance, indicate strong cohort-specific effects, with little linearity in the relationship across cohorts.

To instead identify more consistent asymmetries among the six cohorts, we focused on the 50 most significant leftward (left > right) and 50 most significant rightward (right > left) asymmetric regions from each cohort, out of the 615 atlas regions. We asked whether regions comprising the top leftward and top rightward asymmetries from one cohort showed a similar asymmetry pattern when evaluated in a second, independent cohort. We found this to be the case in more than 75% of cross-cohort comparisons (**Fig. 1D-E**). To then overcome the challenge that these top regions inherently vary across cohorts due to cohort-specific effects, we performed a leave-one-out cross-validation. We reasoned that the average asymmetry pattern of several cohorts together is likely to provide a more reproducible set of results than any one cohort individually. To do this, we averaged the summary pattern of asymmetry from each of five cohorts and compared the resulting values to the remaining sixth cohort. For five of the six possible combinations of cohorts, the top 50 leftward and top 50 rightward asymmetries, defined using the five-cohort average, significantly predicted the pattern of asymmetry in the remaining sixth cohort (**Fig. 1F**). The last combination showed a non-significant trend in the expected direction (likely non-significant due to the high rate of tissue defects present in the images from that study, combined with its low number of animals). This result means that on five of six unique occasions, the top asymmetries obtained through a five-cohort average generalized well to the remaining sixth cohort. By then taking the average asymmetry of all six cohort summaries together, we obtained a final, high-confidence description of asymmetries which are generalizable across independent cohorts.

We lastly confirmed that this result extended to new data by identifying a seventh, previously un-analyzed cohort of animals from a publicly available data repository. We found that our final six-cohort average successfully and significantly predicted the pattern of asymmetry in this seventh previously un-used cohort (**Fig. 1G**). The magnitude of the most significant asymmetries in the six-cohort average ranges from 0.5% to 2.6% difference in regional volume between sides (**Fig. 1H**). The biological implications of this asymmetry pattern are explored in **Fig. 4-7**, after the control experiments presented next (**Fig. 2-3**).

Brain Asymmetry in Mice Is Not Due to Technical Artifacts or Biases. We next performed extensive controls to ensure that our results were not due to technical artefacts or biases. To first validate that our morphometry analysis can recapitulate previously reported results in a non-asymmetry context, we used the same volume data generated above to calculate regional male-female differences in volume (**Fig. 2A**). Previous studies in mice have defined a clear signature of male-female neuroanatomical differences – a larger bed nuclei stria terminalis, medial amygdala, and medial preoptic area in males[81–83] – which we utilized as a positive control analysis. We found that male-female differences are highly reproducible across all 6 original cohorts, and we identified this expected regional signature as the top result (**Fig. 2B-G**). Additionally, we quantitatively compared our data to previous results by Elkind et al. 2023[81] who used one of the same cohorts as us (AMBCA). For this cohort, our results were consistent with theirs, both for sex differences as well as for asymmetry (**Fig. 2H-I, Fig. S2**), despite our groups using independent pipelines. Overall, these analyses confirm that our pipeline is recapitulating established results.

We next investigated whether any modality-specific factor could falsely drive our asymmetry results. To do this, we generated MRI-specific and STPT-specific average asymmetry patterns. We found that the set of top asymmetries defined in one modality significantly predicted asymmetry in the other (**Fig. 3A-B**). Thus, asymmetry generalizes between two fundamentally

distinct image modalities and is not a product of any MRI-specific or STPT-specific artifact – such as *ex cranio* (STPT) vs *in cranio* (MRI) imaging or the MRI-specific steps of our pipeline.

To investigate the potential for biases in the pipeline, we reversed the left-right orientation of 1 STPT cohort (BICCN) and 1 MRI cohort (POND) and re-ran our analysis. We also generated synthetic symmetrical brain images from these samples – a negative control where asymmetry should be absent. We found that the resulting pattern of asymmetry in the STPT cohort was almost entirely inverted when flipping the left-right orientation of the original, un-processed images (**Fig. 3C**). We similarly found that asymmetries measured from a symmetrized STPT cohort were far smaller than those detected in the original images, but interestingly, were highly significant (**Fig. 3D-E; Fig. S3A**). Nonetheless, this data shows that the asymmetries we detect in our non-symmetrized STPT cohorts depend almost entirely on the image left-right orientation, an important result which demonstrates that there is no left-right bias in the pipeline to drive asymmetries. For the POND cohort, we found that asymmetries also strongly depended on the left-right orientation, as in the STPT cohorts, but with some added noise (**Fig. S3A-D**). This noise likely originates from one of the MRI-specific algorithms we used (likely the N4 intensity inhomogeneity correction step), which, when given a pair of identical but flipped input images, does not produce perfectly flipped output images (**Fig. S3E-F**). However, this effect is not driving the overall asymmetry pattern, as the MRI cohorts still generalize well to the STPT cohorts (**Fig. 3A-B**) – which do not use this MRI-specific algorithm during their processing. Overall, the results indicate that our observed asymmetries depend predominantly on the image left-right orientation and not on pipeline bias.

Finally, we assessed whether our results generalize to a different image registration software – Elastix[79] – which uses a different transformation model from the ANTsPy registration package used above. Re-registering each sample using Elastix revealed a similar pattern of asymmetry to that observed with ANTsPy (**Fig. 3F, Fig. S4**). This result makes the prospect of an overall registration error unlikely and rules out the possibility that asymmetry is a software-specific result. Altogether, our results argue strongly in favor of a population-wide pattern of directional asymmetry existing in the adult mouse brain, robust to numerous biological and technical differences between cohorts, independent pipelines, image modalities, and registration packages.

Top Asymmetries Are Comprised of All Major Anatomical Structures. Having established that anatomical asymmetry is indeed present in the mouse brain, we turned our attention to interpreting the regional pattern of asymmetry. Inspecting the set of top asymmetries reveals a diverse collection of regions spanning each major division of the mouse brain (**Fig. 4A**). We saw significant enrichment of atlas labels within the pons among the top set of asymmetries and a near-significant enrichment of cerebellum structures (**Fig. 4B**). However, outside of these areas, we saw no clear enrichment for any other division of the brain among our top results. Among isocortical labels, we saw no evidence of layer-specific enrichment either (**Fig. 4C**). Thus, excluding the pons and cerebellum, our set of top asymmetries mainly reflects the frequency of these structures expected by chance given their proportion in the CCFv3 atlas.

No Association of Anatomical Asymmetries with Functional Asymmetries. Among the top asymmetric regions, the most asymmetric structure is layer 6b of the infralimbic area, with a 2.6% average rightward asymmetry (**Dataset S1**). The medial pretectal area and locus coeruleus also showed a 2.6% leftward asymmetry. Finding these regions as the top asymmetric structures was unexpected given that no evidence for lateralized function exists at these areas. Interestingly, no auditory cortical regions were found in the set of top asymmetric structures despite robust evidence of functionally asymmetric auditory processing in mice[62–65]. We therefore investigated, using the statistical enrichment approach above, whether our set of top anatomical asymmetries were indeed distinct from known functional asymmetries in mice (**Fig. S5A-B, Table S2**). We found that areas of the mouse brain with strong evidence for asymmetric function showed no association with the top anatomical asymmetries identified here (**Fig. 4D, Fig. S5C, Table S2**). We further saw through leave-one-out cross-validation that these functionally asymmetric regions don't appear to drive the

main effects seen in **Fig. 1F,** as they were less consistent across cohorts than the overall set of top regions (consistent only for 3 of 6 cohorts; **Fig. S5C**). Overall, these analyses suggest that gross anatomical asymmetries seen here are generally distinct from known functional asymmetries in mice.

An Anterior-Posterior Pattern of Volume Asymmetry is Driven by SA but Not CT. Although we did not identify an association with known functional asymmetries, we did observe an anterior-posterior (AP) pattern of asymmetry in which anterior regions are larger on the right and posterior regions are larger on the left (**Fig. 1H)**. This can be seen quantitatively by calculating the 3D centroid of each region from the CCFv3 atlas and plotting the AP component of that centroid against its asymmetry. We observe this pattern both when using the set of top regions or when using all regions in our 6-cohort average (**Fig. S6A, Fig. 5A**). Notably, this result is not restricted to the cortex and the effect is stronger in the 6-cohort average than in any one cohort individually (**Fig. S6B-C, Fig. S7**), this latter point indicating that the AP effect is generally obscured by the cohort-specific patterns. Flipping the left-right orientation of the POND and BICCN images reverses the directionality of the pattern while symmetrizing these images eliminates it (**Fig. S6D-E**). Moreover, this effect is evident in both the STPT- and MRI-specific averages and is also present in our analysis using Elastix (**Fig. S6F-H**). We see no evidence of a similar trend for the dorsal-ventral (DV) or medial-lateral (ML) axes (**Fig. 5B, S5I**).

In humans, a CT asymmetry trend exists where anterior regions are thicker on the left and posterior regions are thicker on the right[9,22–24]. To directly assess whether our observations in mice match this reported trend in humans, we measured CT asymmetry directly in all samples. We did this by propagating the CCFv3 cortical labels onto each sample through the reverse registration and applied the Laplacian method[84,85] (**Fig. 5C**; see supplemental methods). Although our AP volume asymmetry pattern is brain-wide, we focused on the cortex here because measurements of thickness are well-defined and because doing so best enables a direct comparison to observations in humans. We found no evidence of a pattern in mice for CT asymmetry with respect to the AP axis (**Fig. 5D**), but we also measured SA asymmetry in parallel and found a highly significant AP gradient in the same direction as our volume asymmetry pattern (**Fig. 5E**). Interestingly this gradient was in the opposite direction of the human CT pattern.

We validated these separate CT and SA measurements by using the hemisphere-specific CT and SA to re-derive volume asymmetry for each cortical territory (layers 1-6b combined into a single label per cortical area). This re-derived volume asymmetry was strongly correlated with our original volume asymmetries measured from the forward registration (**Fig. 5F**), confirming the accuracy of our measurements. Altogether, this data indicates that an AP volume asymmetry pattern exists in mice and is driven by SA asymmetries, but not CT.

Positional Asymmetries but No Cerebral Petalia Exists in Mice. Given that we observe an AP pattern of asymmetry in mice, we wondered whether this indicated a cerebral petalia-like effect. In humans, the right hemisphere protrudes ahead of the left in a brain-wide “twisting” or “warping” pattern[13–17]. Roughly two-thirds of individuals show this trend while the remaining one-third show a reversal or near-symmetry[17]. To examine this in mice, we implemented an automated approach based on recent large-scale papers measuring the petalia in humans and chimpanzees[13,14]. To aid in interpreting our results, we also applied this analysis to 4 cohorts of human subjects (positive controls) and 6 cohorts of non-human primates (NHPs; negative controls) consisting of chimpanzees, macaques, and marmosets (2 cohorts each; **Table S3**). We note that while the presence of a significant petalia in NHPs is controversial, studies agree that such an effect, if present, is much smaller in magnitude and of a weaker frequency in that species' population than in humans[13,17,86,87].

In humans, we found a significant right-frontal protrusion of 0.24% and a significant left-occipital protrusion of 0.70%. Both are normalized by the length of the left hemisphere and are consistent with established findings (**Fig. 6A-B**). In NHPs, we saw a significant right-frontal protrusion as well, but which was significantly smaller than in humans by approximately 3-fold

(0.07% overall; **Fig. 6A**). In contrast, we saw no significant occipital protrusion in NHPs (**Fig. 6B**). In mice, we saw no significant protrusion for either end of the AP axis, with average measurements similar to the NHPs (anterior = 0.06%, posterior = 0.07%; **Fig. 6A-B**). Thus, our measurements do not support the existence of an AP protrusion of one hemisphere with respect to the other in mice (e.g. a cerebral petalia).

However, we reasoned that a more sensitive approach to detecting such an effect would be to leverage the statistical power of many annotated brain regions together, rather than measuring only one region at each end of the cerebrum. We thus measured positional asymmetries for all the CCFv3 regions within each mouse brain. We did this by calculating the 3D centroids for each annotated brain region as mapped onto that animal during the preceding petalia analysis and performed cross-validation using the different cohorts. Here, we asked whether the volume of *many* brain regions was shifted between sides in an AP direction. We found highly reproducible left-right asymmetries of AP position in mice across all 6 of our cohorts (**Fig. 6C**). Regions within the cerebral hemisphere were consistently shifted anteriorly on the right side while regions within the brainstem and cerebellum were shifted anteriorly on the left side (**Fig. 6D-E**). Thus, while no significant AP protrusion asymmetry exists at the mouse cortical poles, reproducible shifts exist between sides at the brain-wide level which match the AP volume and SA gradients.

Evolutionary Context of Mouse Brain Volume Asymmetries. We lastly examined to what degree, if any, our observed volume asymmetries in mice were consistent with those of humans and NHPs. Initial inspection of the overall asymmetry pattern in each species revealed sharp species differences (**Fig. 7A**) as well as cohort-specific asymmetries for marmosets and macaques, like those seen in mice (**Fig. 7B, Fig. S8**). To compare the pattern of asymmetry quantitatively across species, we utilized the cross-species atlas annotations from Garrin et al. 2022[88], the marmoset and macaque cohorts used earlier, and human volume asymmetry data from the Roe et al. 2023 paper[9]. The 2 chimpanzee cohorts from the previous section were excluded for technical reasons (see methods). We found weak correlations in the region-wise asymmetry pattern between any of the species analyzed, using either cytoarchitecturally matched (Brodmann) regions or whole cortical lobes with composite subcortical structures (**Fig. 7C-D**). We similarly found no indication of an AP pattern for volume asymmetry in marmosets or macaques, but interestingly, we found an AP pattern in humans in the opposite direction of mice (**Fig. 8S**) – consistent with the CT asymmetry pattern of humans. Overall, our data indicates anatomical asymmetry to be species-specific.

Discussion

Anatomical asymmetry is a significant feature of the human brain, yet its cellular and developmental basis remains poorly understood. This knowledge gap stems mainly from a lack of mammalian animal models in which mechanistic studies can be more easily pursued. Through our work, we identified an anterior-posterior pattern of volume and SA asymmetry in mice, for which anterior regions are larger and have more surface area on the right, while posterior regions are larger and have more surface area on the left. The cerebral hemisphere as a whole is shifted anteriorly on the right while the brainstem and cerebellum are shifted anteriorly on the left. Cross-cohort validation and extensive control experiments demonstrate our results, though small in magnitude, are consistent in 6 of 7 groups of animals, are free of pipeline bias, and are independent of image modality and analysis software. Our data collectively indicates that a genuine, brain-wide signature of anatomical asymmetry exists in the adult mouse brain.

Considering our results in the context of humans, our findings best align with the idea of a cerebral petalia-like effect in mice, rather than the distinct local asymmetries reported in humans. Our set of 100 top asymmetries largely reflects the above anterior-posterior pattern**.** In this context, it makes intuitive sense that our top anatomical asymmetries lack an obvious overlap with known functionally asymmetric brain regions. The subtle asymmetries captured by our analysis appear to represent a torsion manifesting across the entire brain, while region-specific asymmetries like those seen in humans or the zebrafish habenula appear to be entirely absent in mice. Notably, a study performed in parallel with ours by a different group observed a similar AP trend in the same direction

as us but using only 1 cohort (POND)[89]. Their analysis agrees well with ours, providing additional evidence in support of our conclusion.

One possible explanation for the emergence of macroscale asymmetries is the molecular chirality of cytoskeletal proteins. A recent GWAS study identified enrichment for tubulin genes as genetic modifiers of anatomical asymmetry in humans[25]. In *Drosophila*, the actin cytoskeleton shows an intrinsic handedness that is sufficient to polarize a cell's anterior-posterior axis and yield whole-organ and whole-organism helical-twisting[90]. Neurite growth cones in rodents have been similarly observed *in vitro* to twist in a right-screw (clock-wise) direction in a manner dependent on the actin cytoskeleton[91–93], although whether this occurs *in vivo* is unknown. Our observations here are consistent with such a mechanism occurring in mice.

An alternative explanation could be that asymmetry emerges through a subtle timing difference in development between the left and right hemispheres. In humans, cortical folding in the temporal lobe begins 1-2 weeks sooner on the right than on the left[28,94,95], and two recent studies found that transcriptome-wide changes occurring with age in the early fetal brain were slightly more advanced on one side than the other[96,97]. Anatomical asymmetries are theorized to be a "record" of this developmental timing delay[98]. Whether such an effect is occurring in mice remains unknown as does the potential mediator of such a timing delay. However, having mice as a novel animal model of anatomical brain asymmetry can be a powerful tool to investigate this and other hypotheses.

A longstanding area of interest in humans is the relationship between asymmetry of the visceral organs and asymmetry of the brain. While most evidence points toward separate mechanisms conferring asymmetry in these contexts[29–34], one potential exception is the cerebral petalia. In humans, individuals with reversed visceral organ asymmetry (*situs inversus*) show a high frequency of a reversed cerebral petalia[29–32], although the number of subjects studied in this context remains low (22 total over four studies) and more work is needed. This emerging idea is particularly interesting in light of our observation of a similar torsion-like effect in the mouse brain. Furthermore, two studies in mice that reversed visceral organ asymmetry observed the loss of a functional asymmetry in the hippocampus[69,99]. Thus, while most evidence points toward these pathways being largely disconnected, at least in humans, we wonder whether the signature of neuroanatomical asymmetry we observe here would be reversed in mice with *situs inversus*. The rarity of such individuals in humans makes this relationship challenging to interrogate (hence the low number of subjects thus far), but research using our novel signature of neuroanatomical asymmetry in mice would provide a critical datapoint for understanding this relationship.

For future studies attempting to replicate our results, the asymmetry for the top 100 regions can serve as a direct test of replicability by asking the following question: when measured in a new set of animals, do the leftward and rightward asymmetries defined in this study vary significantly from each other in the predicted direction? (e.g. **Fig. 1F**). A significant difference in this context in the predicted direction provides evidence of replication. This approach can also be used for our reported positional asymmetries.

Our focus here on *sets* of asymmetries highlights the probabilistic nature of our results. The sets of leftward and rightward asymmetries we define are repeatable across independent cohorts, however, individual regions within these sets will undoubtedly show variation in a new cohort. However, defining sets of asymmetric regions ultimately ends up being a strength when applied to future studies: an investigation into the cellular properties of asymmetric regions is likely to be more powerful if the results are applicable over many regions – even with some added noise – rather than in only a few focused regions.

A surprising finding in our study is that highly significant asymmetries exist in most mouse imaging cohorts, but these asymmetry patterns tend to be cohort-specific. Moreover, this is not true for studies of sex differences, where effects in one cohort are readily reproduced in another. Given that this cross-cohort variability is specific to left-right comparisons, we think it is unlikely that it stems from factors which would impact the images equally for both hemispheres: image modality,

number of subjects, or original image resolution, among others. Similarly, biological influences like age, genetic variation, the relative proportion of males and females, and others appear unlikely to be culprits as they have only small effects on human brain asymmetry to begin with[9,22,25,100], and these would impact the images equally for both hemispheres. Instead, technical factors which don't impact both sides equally seem like the most intuitive cause, though future research will need to investigate this to be sure. For STPT samples, causal factors could be the intensity vignetting in the tiled images. For MRI samples, this could be residual shading biases or residual geometric distortion, among other possibilities. In principle, any of these technical factors could create cohort-specific local minima during the registration's optimization process that could trap a more "aggressive" image registration – especially given the small magnitude effects. An alternative explanation could be that husbandry-specific factors drive environment-dependent asymmetries. However, this seems unlikely given that the 2 marmoset cohorts we used showed significant and largely distinct asymmetry patterns but were raised in the same husbandry environment at the same institution (personal communication, acknowledged individual J.H.). Regardless of the source, our cross-cohort approach proved advantageous over a single-cohort analysis as it enabled us to identify this critical issue which should be carefully considered for future studies of anatomical asymmetry outside of humans.

Although we observe no meaningful correlations in asymmetry between species, interpretation of these results should be made cautiously. We observe poor cross-cohort consistency for asymmetry in macaques, and marmosets, so the resulting pattern reflects only the average over these two cohorts, compared to the six cohorts we obtained for mice. Moreover, cross-species comparisons in general are not well-defined and this represents a broader challenge facing the field of neuroimaging. To find similar regions between species, we implemented a curated, atlas-based approach, however, alignment of templates between species using white-matter estimation maps[101] or a common transcriptional space[102] may provide an improvement. Nonetheless, our results align with a previous study which did not observe a major cross-species signature of asymmetry between humans and chimpanzees[24]. Similarly, a study of male-female differences in humans and mice observed weak cross-species agreement, despite robust sex differences in both species[83]. Going forward, additional methods should be explored to further interrogate the question of cross-species comparisons, but at present, major consistency across species seems absent.

As brain-wide mapping studies become easier to perform in small vertebrates, we encourage authors to publish their raw images in open-source repositories like the brain image library[103] or Zenodo.org, along with documentation to identify the left and right hemispheres. The presence in mice of a brain-wide signature of anatomical asymmetry will further enable research into the question of developmental and cellular underpinnings of asymmetry in humans, and publicly available datasets like those used in our study will be invaluable toward this effort.

Overall, we find extensive anatomical asymmetry in the adult mouse brain, manifesting as a brain-wide, anterior-posterior pattern. Our work provides a foundation for future studies to investigate the microscopic basis of this cerebral petalia-like effect in mice.

Materials and Methods

Overall Morphometry Analysis. Our data collection was performed using a series of python, Fiji, and R scripts. Images for each animal were first gathered into a z-stack (if not already) and converted to .tif file format from one of various starting formats (.jpg, .Jp2, .nii, .mnc, .tif). From here, each z-stack was resampled from its original resolution to 50 μm isotropic resolution. MRI samples were skull-stripped followed by N4 bias correction. We then performed image registration (rigid, affine, and non-linear) to align the sample images toward a population-average template (sample image as the moving image; reference template as the fixed image). All templates and atlases were completely left-right symmetrical. From these registrations, we collected the Jacobian determinant field and measured its average value within each CCFv3 atlas region for each sample.

The Jacobian determinant field represents how much the local volume changes at each voxel when transforming one image to align with another. For example, field values of 1.10 or 0.85 at 2 different voxels in the template image indicate that the corresponding volumes in the sample image were 10% larger or 15% smaller respectively than they are in the template image. After calculating average field values for each regions, we then scaled the average field value by the physical size of that region in the original atlas to obtain a volume measurement in μm^3. Extensive details about each cohort, registration settings, processing steps, additional analyses, left-right orientation, and more are provided in **Supplemental Materials and Methods**.

Acknowledgments

We thank numerous members of the neuroimaging community for their generous feedback throughout this project. In this context, we would like to acknowledge Doug Greve, Elisa Guma, Stefan Klein, Yael Balbastre, and Clyde Francks. We would also like to thank individuals who provided critical information related to the left-right orientation or demographics of different cohorts: Gabriel Devenyi, John Sled, Rasmus Birn, Jonathan Oler, Junichi Hata, and Matthew Rushworth. We are thankful to Amit Zeisel for sharing supplemental data from their publication (Elkind et al. 2023[81]). We thank the Harvard Research Computing department for providing early access to the O2portal. We also thank members of the Pourquie lab for thoughtful feedback on the data and manuscript throughout the project.

References

1. Hamada H. Molecular and cellular basis of left-right asymmetry in vertebrates. *Proc Japan Acad Ser B Phys Biol Sci*. 2020;96(7):273-296. doi:10.2183/PJAB.96.021

2. Wade DT, Hewer RL, David RM, Enderby P. Aphasia after stroke: Natural history and associated deficits. *J Neurol Neurosurg Psychiatry*. 1986;49(1):11-16. doi:10.1136/jnnp.49.1.11

3. Packheiser J, Schmitz J, Arning L, Beste C, Güntürkün O, Ocklenburg S. A large-scale estimate on the relationship between language and motor lateralization. *Sci Rep*. 2020;10(1):1-10. doi:10.1038/s41598-020-70057-3

4. Becker E, Karnath HO. Incidence of visual extinction after left versus right hemisphere stroke. *Stroke*. 2007;38(12):3172-3174. doi:10.1161/STROKEAHA.107.489096

5. Çiçek M, Deouell LY, Knight RT. Brain activity during landmark and line bisection tasks. 2009;3(May):1-8. doi:10.3389/neuro.09.007

6. Hecaen H, Angelergues R. Agnosia for Faces (Prosopagnosia). *Arch Neurol*. 1962;7(2):92-100. doi:10.1001/archneur.1962.04210020014002

7. Hilliard RD. Hemispheric Laterality Effects on a Facial Recognition Task in Normal Subjects. *Cortex*. 1968;9(3):246-258. doi:10.1016/S0010-9452(73)80002-4

8. Rossion B, Hanseeuw B, Dricot L. Defining face perception areas in the human brain: A large-scale factorial fMRI face localizer analysis. *Brain Cogn*. 2012;79(2):138-157. doi:10.1016/j.bandc.2012.01.001

9. Roe JM, Vidal-Piñeiro D, Amlien IK, et al. Tracing the development and lifespan change of population-level structural asymmetry in the cerebral cortex. *Elife*. 2023;12:1-32. doi:10.7554/eLife.84685

10. Goldberg E, Roediger D, Kucukboyaci NE, et al. Hemispheric asymmetries of cortical volume in the human brain. *Cortex*. 2013;49(1):200-210. doi:10.1016/j.cortex.2011.11.002

11. Chi JG, Dooling EC, Gilles FH. Left-Right Asymmetries of the Temporal Speech Areas of the Human Fetus. *Arch Neurol*. 1977;34(6):346-348. doi:10.1001/archneur.1977.00500180040008

12. Kertesz A, Geschwind N. Patterns of Pyramidal Decussation and Their Relationship to Handedness. *Arch Neurol*. 1971;24(4):326-332. doi:10.1001/archneur.1971.00480340058006

13. Xiang L, Crow T, Roberts N. Cerebral torque is human specific and unrelated to brain size. *Brain Struct Funct*. 2019;224(3):1141-1150. doi:10.1007/s00429-018-01818-0

14. Zhao L, Matloff W, Shi Y, Cabeen RP, Toga AW. Mapping Complex Brain Torque Components and Their Genetic Architecture and Phenomic Associations in 24,112 Individuals. *Biol Psychiatry*. 2022;91(8):753-768. doi:10.1016/j.biopsych.2021.11.002

15. Bear D, Schiff D, Saver J, Greenberg M, Freeman R. Quantitative Analysis of Cerebral Asymmetries: Fronto-occipital Correlation, Sexual Dimorphism and Association with Handedness. *Arch Neurol*. 1986;43(6):598-603. doi:10.1001/archneur.1986.00520060060019

16. Balzeau A, Gilissen E, Grimaud-Hervé D. Shared pattern of endocranial shape asymmetries among great apes, anatomically modern humans, and fossil hominins. *PLoS One*. 2012;7(1):1-10. doi:10.1371/journal.pone.0029581

17. Kong XZ, Postema M, Schijven D, et al. Large-Scale Phenomic and Genomic Analysis of Brain Asymmetrical Skew. *Cereb Cortex*. 2021;31(9):4151-4168. doi:10.1093/cercor/bhab075

18. Greve DN, Van der Haegen L, Cai Q, et al. A Surface-based Analysis of Language Lateralization and Cortical Asymmetry. *J Cogn Neurosci*. 2013;25(9):1477-1492. doi:10.1162/jocn_a_00405

19. Guadalupe T, Kong XZ, Akkermans SEA, Fisher SE, Francks C. Relations between hemispheric asymmetries of grey matter and auditory processing of spoken syllables in 281 healthy adults. *Brain Struct Funct*. 2022;227(2):561-572. doi:10.1007/s00429-021-02220-z

20. Josse G, Kherif F, Flandin G, Seghier ML, Price CJ. Predicting language lateralization from gray matter. *J Neurosci*. 2009;29(43):13516-13523. doi:10.1523/JNEUROSCI.1680-09.2009

21. Jansen A, Liuzzi G, Deppe M, et al. Structural correlates of functional language dominance: A voxel-based morphometry study: Experimental laboratory research. *J Neuroimaging*. 2010;20(2):148-156. doi:10.1111/j.1552-6569.2009.00367.x

22. Kong XZ, Mathias SR, Guadalupe T, et al. Mapping cortical brain asymmetry in 17,141 healthy individuals worldwide via the ENIGMA consortium. *Proc Natl Acad Sci U S A*. 2018;115(22):E5154-E5163. doi:10.1073/pnas.1718418115

23. Plessen KJ, Hugdahl K, Bansal R, Hao X, Peterson BS. Sex, age, and cognitive correlates of asymmetries in thickness of the cortical mantle across the life span. *J Neurosci*.

2014;34(18):6294-6302. doi:10.1523/JNEUROSCI.3692-13.2014

24. Xiang L, Crow TJ, Hopkins WD, Roberts N. Comparison of Surface Area and Cortical Thickness Asymmetry in the Human and Chimpanzee Brain. Published online 2020:1-15. doi:10.1093/cercor/bhaa202

25. Sha Z, Schijven D, Carrion-Castillo A, et al. The genetic architecture of structural left–right asymmetry of the human brain. *Nat Hum Behav*. Published online 2021. doi:10.1038/s41562-021-01069-w

26. Cuellar-Partida G, Tung JY, Eriksson N, et al. Genome-wide association study identifies 48 common genetic variants associated with handedness. *Nat Hum Behav*. Published online 2020. doi:10.1038/s41562-020-00956-y

27. Wada JA. Cerebral Hemispheric Asymmetry in Humans. *Arch Neurol*. 1975;32(4):239. doi:10.1001/archneur.1975.00490460055007

28. Kasprian G, Langs G, Brugger PC, et al. The prenatal origin of hemispheric asymmetry: An in utero neuroimaging study. *Cereb Cortex*. 2011;21(5):1076-1083. doi:10.1093/cercor/bhq179

29. Vingerhoets G, Li X, Hou L, et al. Brain structural and functional asymmetry in human situs inversus totalis. *Brain Struct Funct*. 2018;223(4):1937-1952. doi:10.1007/s00429-017-1598-5

30. Kennedy DN, O'Craven KM, Ticho BS, Goldstein AM, Makris N, Henson JW. Structural and functional brain asymmetries in human situs inversus totalis. *Neurology*. 1999;53(6):1260-1265. doi:10.1212/wnl.53.6.1260

31. Schuler AL, Kasprian G, Schwartz E, et al. Mens inversus in corpore inverso? Language lateralization in a boy with situs inversus totalis. *Brain Lang*. 2017;174:9-15. doi:10.1016/j.bandl.2017.06.005

32. Ihara A, Hirata M, Fujimaki N, et al. Neuroimaging study on brain asymmetries in situs inversus totalis. *J Neurol Sci*. 2010;288(1-2):72-78. doi:10.1016/j.jns.2009.10.002

33. Gerrits R, Vingerhoets G. Brain functional segregation, handedness and cognition in situs inversus totalis: A replication study. *Neuropsychologia*. 2023;191:108731. doi:10.1016/j.neuropsychologia.2023.108731

34. Tanaka S, Kanzaki R, Yoshibayashi M, Kamiya T, Sugishita M. Dichotic listening in patients with situs inversus:Brain asymmetry and situs asymmetry. *Neuropsychologia*. 1999;37(7):869-874. doi:10.1016/S0028-3932(98)00144-4

35. Postema MC, van Rooij D, Anagnostou E, et al. Altered structural brain asymmetry in autism spectrum disorder in a study of 54 datasets. *Nat Commun*. 2019;10(1):1-12. doi:10.1038/s41467-019-13005-8

36. Sha Z, Rooij D, Anagnostou E, et al. Subtly altered topological asymmetry of brain structural covariance networks in autism spectrum disorder across 43 datasets from the ENIGMA consortium. 2022;(August 2021). doi:10.1038/s41380-022-01452-7

37. Schijven D, Postema MC, Fukunaga M, et al. Large-scale analysis of structural brain

asymmetries in schizophrenia via the ENIGMA consortium. 2023;120(14):1-12.

38. Sommer I, Aleman A, Ramsey N, Bouma A, Kahn R. Handedness, language lateralisation and anatomical asymmetry in schizophrenia: Meta-analysis. *Br J Psychiatry*. 2001;178(APR.):344-351. doi:10.1192/bjp.178.4.344

39. Concha ML, Russell C, Regan JC, et al. Local Tissue Interactions across the Dorsal Midline of the Forebrain Establish CNS Laterality to the parapineal precursors. Ablation of cells in the left ventral epithalamus can reverse laterality in wild-type embryos and impose the direction of CNS asym-. *Neuron*. 2003;39:423-438.

40. Roussigné M, Bianco IH, Wilson SW, Blader P. Nodal signalling imposes left-right asymmetry upon neurogenesis in the habenular nuclei. *Development*. 2009;136(9):1549-1557. doi:10.1242/dev.034793

41. Lekk I, Duboc V, Faro A, Nicolaou S, Blader P, Wilson SW. Sox1A mediates the ability of the parapineal to impart habenular left-right asymmetry. *Elife*. 2019;8:1-23. doi:10.7554/eLife.47376

42. Pascual A, Huang KL, Neveu J, Préat T. Brain asymmetry and long-term memory. *Nature*. 2004;427(6975):605-606. doi:10.1038/427605a

43. Lapraz F, Boutres C, Fixary-Schuster C, et al. Asymmetric activity of NetrinB controls laterality of the Drosophila brain. *Nat Commun*. 2023;14(1). doi:10.1038/s41467-023-36644-4

44. Hopkins WD, Taglialatela JP, Meguerditchian A, Nir T, Schenker NM, Sherwood CC. Gray matter asymmetries in chimpanzees as revealed by voxel-based morphometry. *Neuroimage*. 2008;42(2):491-497. doi:10.1016/j.neuroimage.2008.05.014

45. Vickery S, Hopkins WD, Sherwood CC, et al. Chimpanzee brain morphometry utilizing standardized mri preprocessing and macroanatomical annotations. *Elife*. 2020;9:1-20. doi:10.7554/eLife.60136

46. Cantalupo C, Hopkins WD. Asymmetric Broca's area in great apes. *Nature*. 2001;414(6863):505-505. doi:10.1038/35107134

47. Keller SS, Roberts N, Hopkins W. A comparative magnetic resonance imaging study of the anatomy, variability, and asymmetry of Broca's area in the human and chimpanzee brain. *J Neurosci*. 2009;29(46):14607-14616. doi:10.1523/JNEUROSCI.2892-09.2009

48. Hopkins WD, Misiura M, Pope SM, Latash EM. Behavioral and brain asymmetries in primates: a preliminary evaluation of two evolutionary hypotheses. *Ann N Y Acad Sci*. 2015;1359(1):65-83. doi:10.1111/nyas.12936

49. Kim J, Jung Y, Barcus R, et al. Rhesus Macaque Brain Developmental Trajectory: A Longitudinal Analysis Using Tensor-Based Structural Morphometry and Diffusion Tensor Imaging. *Cereb Cortex*. 2020;30(8):4325-4335. doi:10.1093/cercor/bhaa015

50. Xia J, Wang F, Wu Z, et al. Mapping hemispheric asymmetries of the macaque cerebral cortex during early brain development. *Hum Brain Mapp*. 2020;41(1):95-106. doi:10.1002/hbm.24789

51. Hopkins WD, Avants BB. Regional and hemispheric variation in cortical thickness in chimpanzees (Pan troglodytes). *Ann Intern Med*. 2013;158(6):5241-5248. doi:10.1523/JNEUROSCI.2996-12.2013

52. Gannon PJ, Holloway RL, Broadfield DC, Braun AR. Asymmetry of chimpanzee planum temporale: Humanlike pattern of Wernicke's brain language area homolog. *Science (80-)*. 1998;279(5348):220-222. doi:10.1126/science.279.5348.220

53. Hopkins WD, Marino L, Rilling JK, MacGregor LA. Planum temporale asymmetries in great apes as revealed by magnetic resonance imaging (MRI). *Neuroreport*. 1998;9(12):2913-2918. doi:10.1097/00001756-199808240-00043

54. Cantalupo C, Pilcher DL, Hopkins WD. Are planum temporale and sylvian fissure asymmetries directly related? A MRI study in great apes. *Neuropsychologia*. 2003;41(14):1975-1981. doi:10.1016/S0028-3932(02)00288-9

55. Hopkins WD, Nir TM. Planum temporale surface area and grey matter asymmetries in chimpanzees (Pan troglodytes): The effect of handedness and comparison with findings in humans. *Behav Brain Res*. 2010;208(2):436-443. doi:10.1016/j.bbr.2009.12.012

56. Marie D, Roth M, Lacoste R, et al. Left Brain Asymmetry of the Planum Temporale in a Nonhominid Primate: Redefining the Origin of Brain Specialization for Language. *Cereb Cortex*. 2018;28(5):1808-1815. doi:10.1093/cercor/bhx096

57. Becker Y, Sein J, Velly L, et al. Early Left-Planum Temporale Asymmetry in newborn monkeys (Papio anubis): A longitudinal structural MRI study at two stages of development. *Neuroimage*. 2021;227(July 2020):117575. doi:10.1016/j.neuroimage.2020.117575

58. Becker Y, Meguerditchian A. Structural Brain Asymmetries for Language: A Comparative Approach across Primates. *Symmetry (Basel)*. 2022;14(5):1-21. doi:10.3390/sym14050876

59. Geschwind N, Levitsky W. Human Brain : Left-Right Asymmetries in Temporal Speech Region Published by : American Association for the Advancement of Science Stable URL : http://www.jstor.org/stable/1723941 Human Brain : Left-Right Asymmetries in Temporal Speech Region. 1968;161(3837):186-187.

60. Steinmetz H, Volkmann J, Jäncke L, Freund H -J. Anatomical left-right asymmetry of language-related temporal cortex is different in left- and right-handers. *Ann Neurol*. 1991;29(3):315-319. doi:10.1002/ana.410290314

61. Ellenbroek B, Youn J. Rodent models in neuroscience research: Is it a rat race? *DMM Dis Model Mech*. 2016;9(10):1079-1087. doi:10.1242/dmm.026120

62. Levy RB, Marquarding T, Reid AP, Pun CM, Renier N, Oviedo H V. Circuit asymmetries underlie functional lateralization in the mouse auditory cortex. *Nat Commun*. 2019;10(1). doi:10.1038/s41467-019-10690-3

63. Marlin BJ, Mitre M, D'Amour JA, Chao M V., Froemke RC. Oxytocin enables maternal behaviour by balancing cortical inhibition. *Nature*. 2015;520(7548):499-504. doi:10.1038/nature14402

64. Ehret G. Left hemisphere advantage in the mouse brain for recognizing ultrasonic communication calls. *Nature*. 1987;325(6101):249-251. doi:10.1038/325249a0

65. Neophytou D, Arribas DM, Arora T, Levy RB, Park IM, Oviedo H V. Differences in temporal processing speeds between the right and left auditory cortex reflect the strength of recurrent synaptic connectivity. *PLoS Biol*. 2022;20(10):1-20. doi:10.1371/journal.pbio.3001803

66. Wu Y, Chen C, Chen M, et al. The anterior insular cortex unilaterally controls feeding in response to aversive visceral stimuli in mice. *Nat Commun*. 2020;11(1). doi:10.1038/s41467-020-14281-5

67. El-Gaby M, Reeve HM, Lopes-dos-Santos V, et al. An emergent neural coactivity code for dynamic memory. *Nat Neurosci*. 2021;24(5):694-704. doi:10.1038/s41593-021-00820-w

68. Shipton OA, El-Gaby M, Apergis-Schoute J, et al. Left-right dissociation of hippocampal memory processes in mice. *Proc Natl Acad Sci U S A*. 2014;111(42):15238-15243. doi:10.1073/pnas.1405648111

69. Goto K, Kurashima R, Gokan H, Inoue N, Ito I, Watanabe S. Left-right asymmetry defect in the hippocampal circuitry impairs spatial learning and working memory in IV mice. *PLoS One*. 2010;5(11):1-7. doi:10.1371/journal.pone.0015468

70. Song D, Wang D, Yang Q, et al. The lateralization of left hippocampal CA3 during the retrieval of spatial working memory. *Nat Commun*. 2020;11(1):1-13. doi:10.1038/s41467-020-16698-4

71. Scicli AP, Petrovich GD, Swanson LW, Thompson RF. Contextual Fear Conditioning Is Associated with Lateralized Expression of the Immediate Early Gene c-fos in the Central and Basolateral Amygdalar Nuclei. *Behav Neurosci*. 2004;118(1):5-14. doi:10.1037/0735-7044.118.1.5

72. Kim S, Mátyás F, Lee S, Acsády L, Shin HS. Lateralization of observational fear learning at the cortical but not thalamic level in mice. *Proc Natl Acad Sci U S A*. 2012;109(38):15497-15501. doi:10.1073/pnas.1213903109

73. Zhang MM, Geng AQ, Chen K, et al. Glutamatergic synapses from the insular cortex to the basolateral amygdala encode observational pain. *Neuron*. 2022;110(12):1993-2008.e6. doi:10.1016/j.neuron.2022.03.030

74. Kim SW, Kim M, Baek J, et al. Hemispherically lateralized rhythmic oscillations in the cingulate-amygdala circuit drive affective empathy in mice. *Neuron*. 2023;111(3):418-429.e4. doi:10.1016/j.neuron.2022.11.001

75. Collins RL. On the inheritance of Laterality. *J Hered*. 1968;1(59):9-12. doi:10.1136/bmj.1.2317.1175-a

76. Wang Q, Ding SL, Li Y, et al. The Allen Mouse Brain Common Coordinate Framework: A 3D Reference Atlas. *Cell*. 2020;181(4):936-953.e20. doi:10.1016/j.cell.2020.04.007

77. Avants BB, Epstein CL, Grossman M, Gee JC. Symmetric diffeomorphic image registration with cross-correlation: evaluating automated labeling of elderly and neurodegenerative brain. *Med Image Anal*. 2008;12(1):26-41. doi:10.1016/j.media.2007.06.004

78. Tustison NJ, Cook PA, Holbrook AJ, et al. The ANTsX ecosystem for quantitative biological and medical imaging. *Sci Rep*. 2021;11(1):9068. doi:10.1038/s41598-021-87564-6

79. Klein S, Staring M, Murphy K, Viergever MA, Pluim JPW. elastix : A Toolbox for Intensity-Based Medical Image Registration. 2010;29(1):196-205.

80. Spring S, Lerch JP, Wetzel MK, Evans AC, Henkelman RM. Cerebral asymmetries in 12-week-old C57Bl/6J mice measured by magnetic resonance imaging. *Neuroimage*. 2010;50(2):409-415. doi:10.1016/j.neuroimage.2009.12.043

81. Elkind D, Hochgerner H, Aloni E, Shental N, Zeisel A. Sex, strain, and lateral differences in brain cytoarchitecture across a large mouse population. *Elife*. 2023;12:1-21. doi:10.7554/eLife.82376

82. Qiu LR, Fernandes DJ, Szulc-Lerch KU, et al. Mouse MRI shows brain areas relatively larger in males emerge before those larger in females. *Nat Commun*. 2018;9(1). doi:10.1038/s41467-018-04921-2

83. Guma E, Beauchamp A, Liu S, et al. Comparative neuroimaging of sex differences in human and mouse brain anatomy. Published online 2023. https://doi.org/10.1101/2023.08.23.554334

84. Jones SE, Buchbinder BR, Aharon I. Three-dimensional mapping of cortical thickness using Laplace's equation. *Hum Brain Mapp*. 2000;11(1):12-32. doi:10.1002/1097-0193(200009)11:1<12::AID-HBM20>3.0.CO;2-K

85. Lerch JP, Carroll JB, Dorr A, et al. Cortical thickness measured from MRI in the YAC128 mouse model of Huntington's disease. *Neuroimage*. 2008;41(2):243-251. doi:10.1016/j.neuroimage.2008.02.019

86. Holloway RL, De La Costelareymondie MC. Brain endocast asymmetry in pongids and hominids: Some preliminary findings on the paleontology of cerebral dominance. *Am J Phys Anthropol*. 1982;58(1):101-110. doi:10.1002/ajpa.1330580111

87. Fears SC, Scheibel K, Abaryan Z, et al. Anatomic brain asymmetry in vervet monkeys. *PLoS One*. 2011;6(12):1-10. doi:10.1371/journal.pone.0028243

88. Garin CM, Garin M, Silenzi L, Jaffe R, Constantinidis C. Multilevel atlas comparisons reveal divergent evolution of the primate brain. *Proc Natl Acad Sci U S A*. 2022;119(25):1-9. doi:10.1073/pnas.2202491119

89. Rivera-Olvera A, Houwing DJ, Ellegood J, et al. The universe is asymmetric, the mouse brain too. *bioRxiv*. Published online 2023:2023.09.01.555907. https://www.biorxiv.org/content/10.1101/2023.09.01.555907v1%0Ahttps://www.biorxiv.org/content/10.1101/2023.09.01.555907v1.abstract

90. Lebreton G, Géminard C, Lapraz F, et al. Molecular to organismal chirality is induced by the conserved myosin 1D. *Science (80-)*. 2018;362(6417):949-952. doi:10.1126/science.aat8642

91. Tamada A, Kawase S, Murakami F, Kamiguchi H. Autonomous right-screw rotation of growth cone filopodia drives neurite turning. *J Cell Biol*. 2010;188(3):429-441. doi:10.1083/jcb.200906043

92. Heacock AM, Agranoff BW. Clockwise growth of neurites from retinal explants. *Science*. 1977;198(4312):64-66. doi:10.1126/science.897684

93. Romijn HJ, Mud MT, Wolters PS, Corner MA. Neurite formation in dissociated cerebral cortex in vitro: evidence for clockwise outgrowth and autotopic contacts. *Brain Res*. 1980;192(2):575-580. doi:10.1016/0006-8993(80)90910-5

94. Chi JG, Dooling EC, Gilles FH. Gyral development of the human brain. *Ann Neurol*. 1977;1(1):86-93. doi:10.1002/ana.410010109

95. Dubois J, Benders M, Cachia A, et al. Mapping the early cortical folding process in the preterm newborn brain. *Cereb Cortex*. 2008;18(6):1444-1454. doi:10.1093/cercor/bhm180

96. de Kovel CGF, Lisgo S, Karlebach G, et al. Left–Right Asymmetry of Maturation Rates in Human Embryonic Neural Development. *Biol Psychiatry*. 2017;82(3):204-212. doi:10.1016/j.biopsych.2017.01.016

97. de Kovel CGF, Lisgo SN, Fisher SE, Francks C. Subtle left-right asymmetry of gene expression profiles in embryonic and foetal human brains. *Sci Rep*. 2018;8(1):1-13. doi:10.1038/s41598-018-29496-2

98. Best CT. The emergence of cerebral asymmetries in early human development: A literature review and a neuroembryological model. *Brain Lateralization Child Dev Implic*. 1988;88:5-34.

99. Kawakami R, Dobi A, Shigemoto R, Ito I. Right isomerism of the brain in inversus viscerum mutant mice. *PLoS One*. 2008;3(4):1-6. doi:10.1371/journal.pone.0001945

100. Guadalupe T, Mathias SR, vanErp TGM, et al. Human subcortical brain asymmetries in 15,847 people worldwide reveal effects of age and sex. *Brain Imaging Behav*. 2017;11(5):1497-1514. doi:10.1007/s11682-016-9629-z

101. Eichert N, Robinson EC, Bryant KL, et al. Cross-species cortical alignment identifies different types of anatomical reorganization in the primate temporal lobe. *Elife*. 2020;9:1-30. doi:10.7554/eLife.53232

102. Beauchamp A, Yee Y, Darwin BC, Raznahan A, Mars RB, Lerch JP. Whole-brain comparison of rodent and human brains using spatial transcriptomics. *Elife*. 2022;11:1-24. doi:10.7554/eLife.79418

103. Kenney M, Vasylieva I, Hood G, et al. The Brain Image Library: A Community-Contributed Microscopy Resource for Neuroscientists. *bioRxiv Prepr Serv Biol*. Published online 2024. doi:10.1101/2023.12.22.573024

104. Oh SW, Harris JA, Ng L, et al. A mesoscale connectome of the mouse brain. *Nature*. 2014;508(7495):207-214. doi:10.1038/nature13186

105. Hawrylycz M, Martone ME, Ascoli GA, et al. A guide to the BRAIN Initiative Cell Census Network data ecosystem. *PLoS Biol*. 2023;21(6 June):1-30. doi:10.1371/journal.pbio.3002133

106. Newmaster KT, Nolan ZT, Chon U, et al. Quantitative cellular-resolution map of the oxytocin receptor in postnatally developing mouse brains. *Nat Commun*. 2020;11(1):1-12.

doi:10.1038/s41467-020-15659-1

107. Ellegood J, Anagnostou E, Babineau BA, et al. Clustering autism: using neuroanatomical differences in 26 mouse models to gain insight into the heterogeneity. *Mol Psychiatry*. 2015;20(1):118-125. doi:10.1038/mp.2014.98

108. Guma E, Bordignon P do C, Devenyi GA, et al. Early or Late Gestational Exposure to Maternal Immune Activation Alters Neurodevelopmental Trajectories in Mice: An Integrated Neuroimaging, Behavioral, and Transcriptional Study. *Biol Psychiatry*. 2021;90(5):328-341. doi:10.1016/j.biopsych.2021.03.017

109. Nugent AC, Thomas AG, Mahoney M, et al. The NIMH intramural healthy volunteer dataset: A comprehensive MEG, MRI, and behavioral resource. *Sci Data*. 2022;9(1):1-10. doi:10.1038/s41597-022-01623-9

110. Nárai Á, Hermann P, Auer T, et al. Movement-related artefacts (MR-ART) dataset of matched motion-corrupted and clean structural MRI brain scans. *Sci Data*. 2022;9(1):1-6. doi:10.1038/s41597-022-01694-8

111. Wei D, Zhuang K, Ai L, et al. Data Descriptor: Structural and functional brain scans from the cross-sectional Southwest University adult lifespan dataset. *Sci Data*. 2018;5:1-10. doi:10.1038/sdata.2018.134

112. Noonan MAP, Sallet J, Mars RB, et al. A Neural Circuit Covarying with Social Hierarchy in Macaques. *PLoS Biol*. 2014;12(9). doi:10.1371/journal.pbio.1001940

113. Hata J, Nakae K, Tsukada H, et al. Multi-modal brain magnetic resonance imaging database covering marmosets with a wide age range. *Sci Data*. 2023;10(1):1-8. doi:10.1038/s41597-023-02121-2

114. Skibbe H, Rachmadi MF, Nakae K, et al. *The Brain/MINDS Marmoset Connectivity Resource: An Open-Access Platform for Cellular-Level Tracing and Tractography in the Primate Brain*. Vol 21.; 2023. doi:10.1371/journal.pbio.3002158

115. Kirst C, Skriabine S, Vieites-Prado A, et al. Mapping the Fine-Scale Organization and Plasticity of the Brain Vasculature. *Cell*. 2020;180(4):780-795.e25. doi:10.1016/j.cell.2020.01.028

116. Huang CC, Rolls ET, Feng J, Lin CP. An extended Human Connectome Project multimodal parcellation atlas of the human cortex and subcortical areas. *Brain Struct Funct*. 2022;227(3):763-778. doi:10.1007/s00429-021-02421-6

117. Dale AM, Fischl B, Sereno MI. Cortical surface-based analysis. I. Segmentation and surface reconstruction. *Neuroimage*. 1999;9(2):179-194. doi:10.1006/nimg.1998.0395

118. Glasser MF, Coalson TS, Robinson EC, et al. A multi-modal parcellation of human cerebral cortex. *Nature*. 2016;536(7615):171-178. doi:10.1038/nature18933

Figures and Tables

Figure 1. Reproducible Region-Wise Asymmetry Patterns in the Adult Mouse Brain.

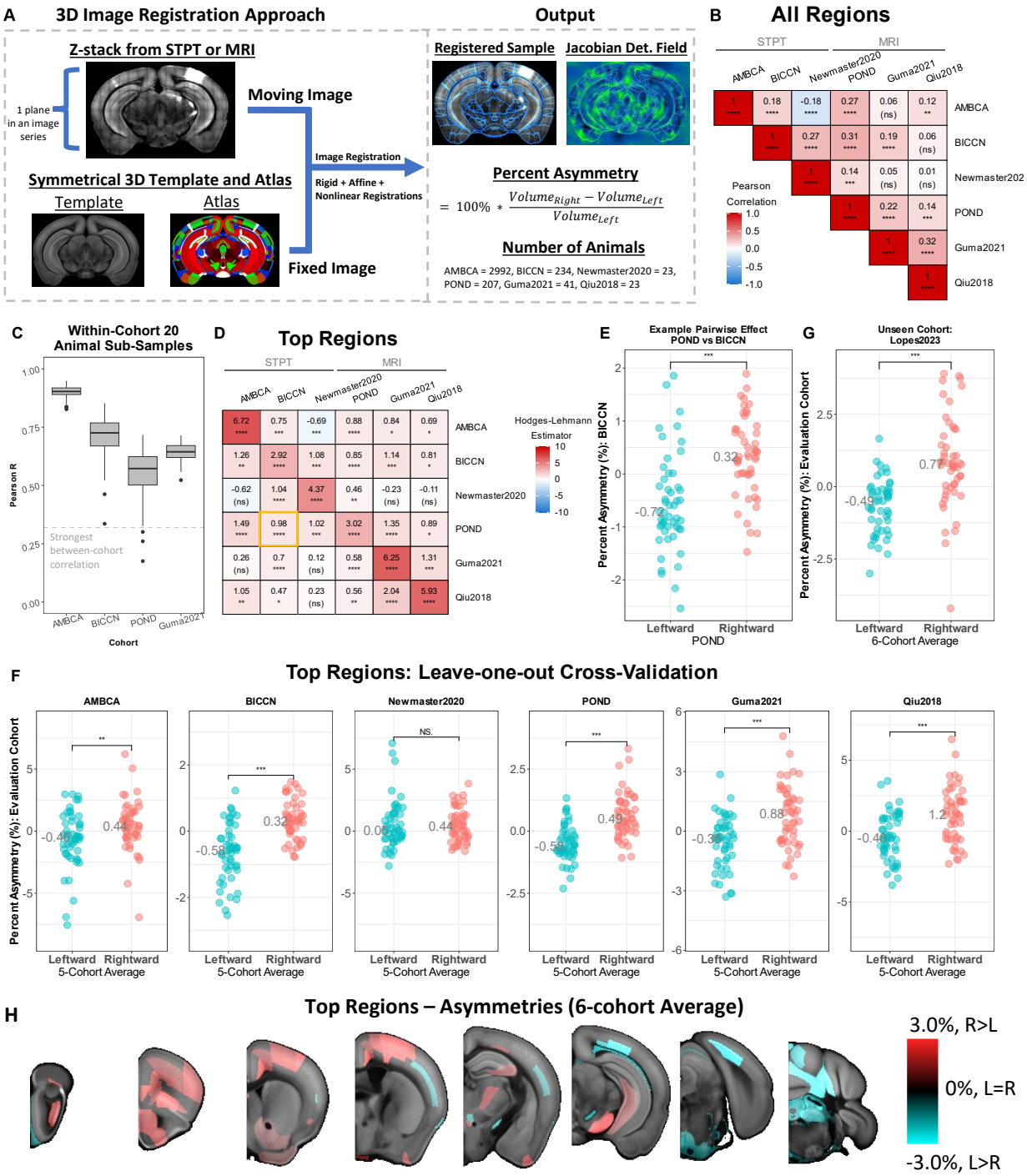

Figure 1. A) Experimental workflow. **B)** Matrix of region-wise asymmetry comparisons between cohorts for all brain regions. Cell value is Pearson correlation between the 2 cohorts for asymmetry of all regions. Second line in cell indicates significance of the correlation. **C)** Distribution of Pearson R values from sub-sampling 20 animals and comparing the sub-sampled asymmetry pattern with either the full cohort (AMBCA,BICCN,POND), or the remaining 21 animals (Guma2021). Dashed line is largest non-diagonal value in B). **D)** Matrix of region-wise asymmetry comparisons between datasets using top 50 leftward and top 50 rightward regions. Cell value is the median of differences (Hodges-lehmann estimator). Top regions are defined in the cohort along the row and then evaluated using the cohort in the column. Gold rectangle is example shown in E). **E)** Example of top regions categorical scatter plot. Each point is 1 brain region. Top regions were defined using the POND dataset and evaluated using the BICCN dataset. Value indicates the median asymmetry in the evaluation cohort for that set of brain regions. **F)** Leave-one-out analysis where title of plot indicates which cohort was left-out and used as the evaluation cohort. Top regions were defined using each 5-cohort average. **G)** Evaluation of 6-cohort average in previously un-tested Lopes2023 cohort (n = 48 animals). **H)** Montage of top 100 regional asymmetries in the 6-cohort average pattern. **D-G)** Statistics are Wilcoxon rank-sum test. * is $p < 0.05$; ** is $p < 0.01$; *** is $p < 0.001$; **** is $p < 0.0001$.

Figure 2. Same Jacobian Maps Reveal Highly Reproducible and Established Sex Differences.

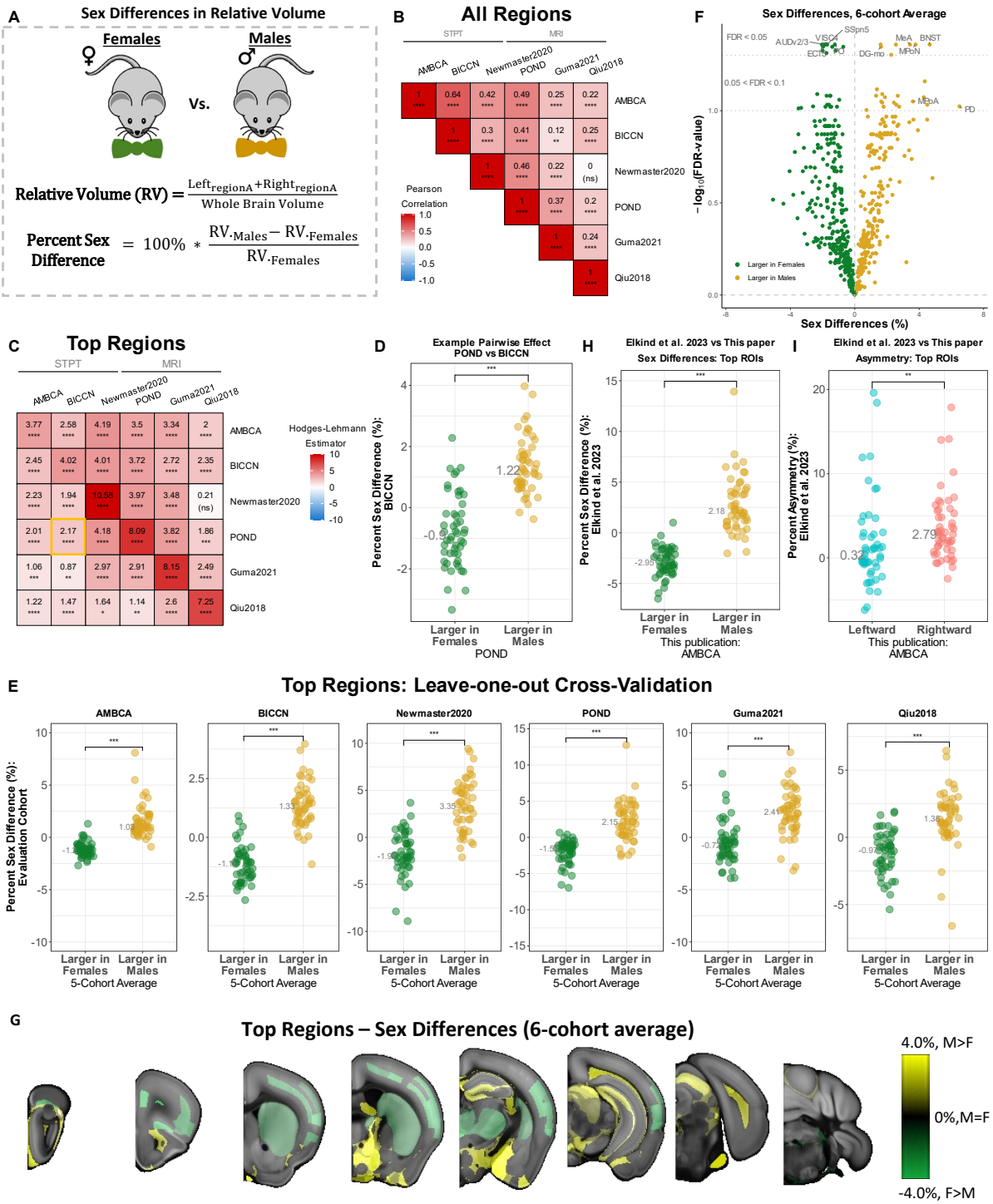

Figure 2. A) Experimental overview. **B)** Matrix of region-wise sex-difference comparisons between cohorts for all regions. **C)** Matrix of region-wise sex-difference comparisons between cohorts using top 50 male-larger and top 50 female-larger regions. Value is median of differences (Hodges-lehmann estimator). Top regions are defined from the cohort along the row and are then evaluated using the cohort in the column. Gold rectangle is example in D. **D)** Example of top regions categorical scatter plot highlighted by gold rectangle in C). Each point is 1 brain region. Top regions were defined using the POND dataset and evaluated using the BICCN dataset. Values indicates the median sex difference in the evaluation cohort for that set of brain regions. **E)** Leave-one-out analysis where title of plot indicates which cohort was left-out and used as the evaluation cohort. Top regions were defined using each 5-cohort average. **F)** Volcano plot of significant sex differences using 6-cohort average. **G)** Montage of top regional sex differences in the 6-cohort average pattern. **H-I)** Comparison of this publication's AMBCA **H)** sex differences and **I)** asymmetries to results of Elkind et al. 2023, who used the AMBCA as well. **C-E, H-I)** Statistics are Wilcoxon rank-sum test. * is $p < 0.05$; ** is $p < 0.01$; *** is $p < 0.001$; **** is $p < 0.0001$.

Figure 3. Asymmetries Are Not Due to Technical Artefacts or Biases.

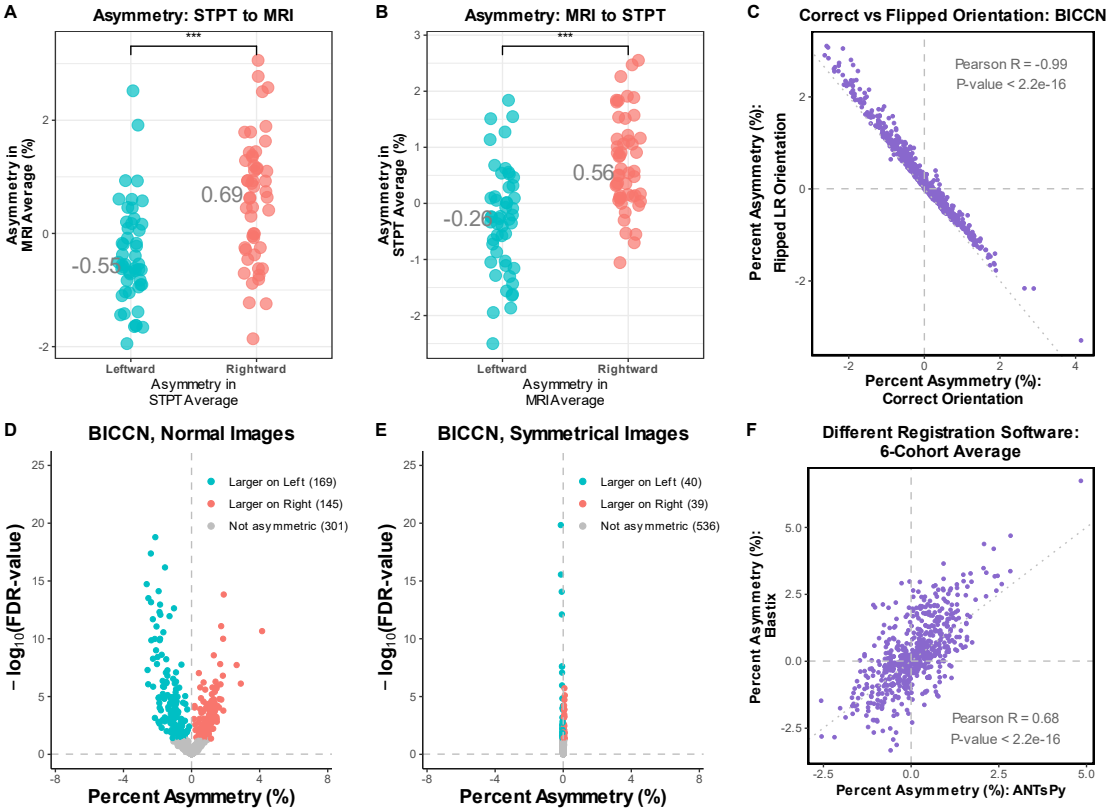

Figure 3. A) Comparison of STPT-specific average asymmetry pattern (X-axis) in the MRI-specific average (Y-axis) using top regions. **B)** Comparison of MRI-specific average asymmetry pattern (X-axis) in STPT-specific average (Y-axis) using top regions. **A-B)** Statistics are Wilcoxon rank-sum test. *** is $p < 0.001$. **C)** Comparison of BICCN region-wise asymmetry pattern between original and left-right reversed images. Each point is a brain region where the value is the mean asymmetry for that region across all animals in each analysis. **D-E)** Volcano plot of asymmetry for BICCN cohort where each point is a brain region. **D)** Analysis using normal images (same as **Fig S1B**). **E)** Analysis using synthetically symmetrized samples. **F)** Comparison of region-wise asymmetry pattern in 6-cohort average between ANTsPy and Elastix.

Figure 4. Characterization of Volume Asymmetry Pattern in the Adult Mouse Brain.

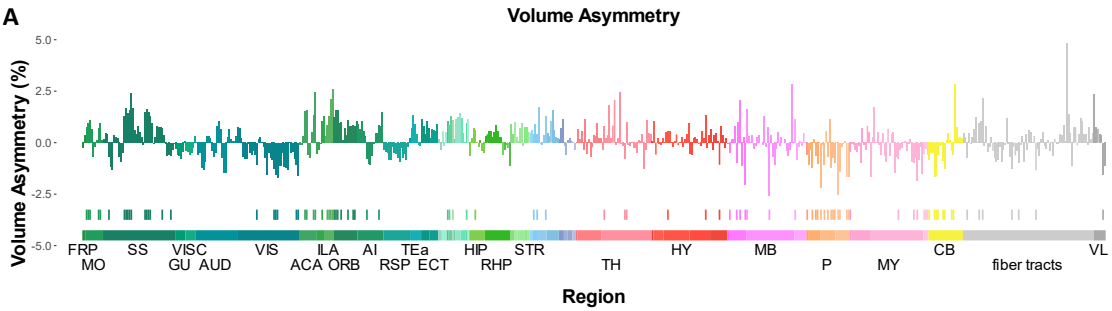

B Enrichment of Anatomical Labels in Top Regions

Division	Odds-Ratio in Top 100	Nominal Composite Asymmetry (%)
Olfactory Areas	1.49	0.11
Isocortex	1.43	0.04
Hippocampal formation	0.20	0.13
Striatum	1.11	0.5
Thalamus	0.34	0.26
Hypothalamus	0.33	0.08
Midbrain	0.83	0.10
Pons	7.42**	-0.58
Medulla	0.92	-0.54
Cerebellum	4.13*	-0.30
White Matter	0.41	-0.04
Ventricular system	0.86	0.81

C Enrichment of Isocortical Layers in Top Regions

Isocortical Layers	Odds-Ratio in Top 100	Nominal Composite Asymmetry (%)
Isocortex Layer 1	0.77	-0.03
Isocortex Layer 2/3	0.77	0.09
Isocortex Layer 4	0.56	0.05
Isocortex Layer 5	2.32	0.10
Isocortex Layer 6a	2.32	-0.07
Isocortex Layer 6b	1.22	-0.26

D Enrichment of Functionally Asymmetric Regions

	Odds-Ratio in Top 100	Nominal Composite Asymmetry (%)
Functionally Asymmetric Regions	1.26	N/A

Figure 4. A) Bar plot of the full Allen CCFv3 where the height of each bar along the X-axis corresponds to the nominal asymmetry in the 6-cohort average. Row of sparse ticks at approximately Y = -3 indicates whether the structure is present in set of top regions derived from the 6-cohort average: presence of tick mark indicates presence of region in top asymmetries, absence of tick mark indicates absence from top asymmetries. Color bar at approximately Y = -4.5 illustrates the broader division of tissue to which that region belongs. **B-D)** Statistical enrichment of regions within **B)** various broad anatomical divisions, **C)** Isocortical layers, or **D)** regions with established functional asymmetries in the set of the top 100 asymmetric brain regions. Nominal asymmetry of the composite structure is included as well. ** indicates a significant enrichment of pons labels in the set of top regions at FDR < 0.05. * indicates near-significant enrichment of cerebellum labels in set of top regions at FDR = 0.054. All others are non-significant. N/A indicates not applicable.

Figure 5. Anterior-Posterior Pattern of Volume Asymmetry is Driven by SA But Not CT.

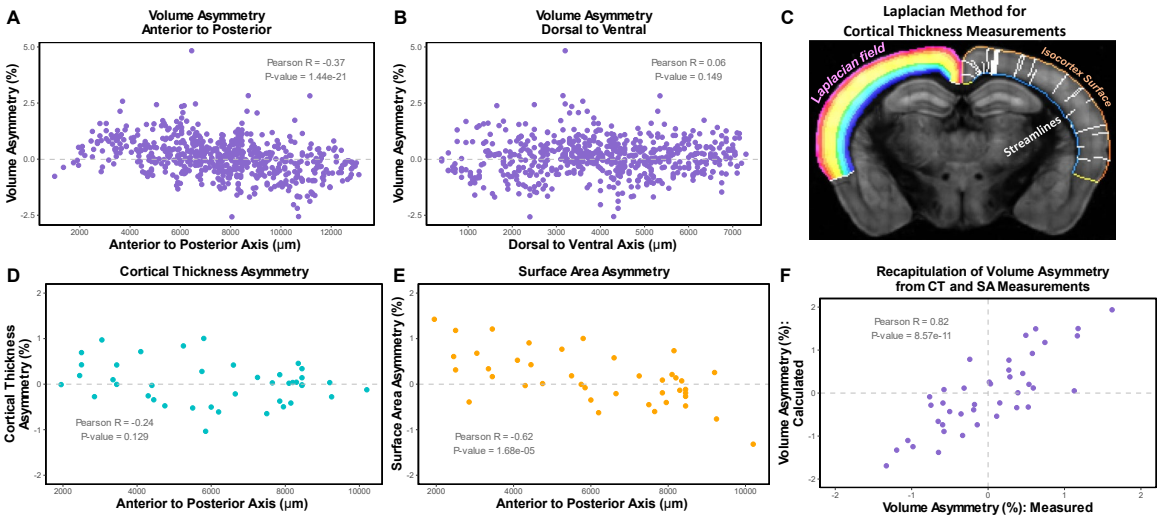

Figure 5. A-B) Average asymmetry of each brain region derived from the 6-cohort average plotted against the **A)** anterior-posterior or **B)** dorsal-ventral position of that region in the atlas. **C)** Illustration of Laplacian Method for calculating cortical thickness, during which surface area can also be collected from the "Isocortex Surface". The cortex is modeled as 3 surfaces: the pial surface ("isocortex surface") or the white matter-grey matter interface (blue line overlaying corpus callosum), and a special cortical geometry surface (yellow line by piriform cortex). A smooth Laplacian field is generated between the pial surface and white matter-grey matter interface. The steepest descent path through the field (streamlines) is generated from each surface pixel to the white matter-grey matter interface. **D)** Average cortical thickness per cortical territory from 6-cohort average (all layers collapsed) calculated using method in C). **E)** Average pial surface area per cortical territory from 6-cohort average. **F)** Comparison of 6-cohort average volume asymmetry per cortical territory (all layers collapsed) measured using original Jacobian-derived volume analysis with volume asymmetry calculated through separate cortical thickness and surface area measurements. In all graphs, each point is 1 brain region and the value is the mean asymmetry for the appropriate metric calculated in the 6-cohort average. All statistics are the significance of the Pearson correlation.

Figure 6. Positional Asymmetries But No Cerebral Petalia in Mice.

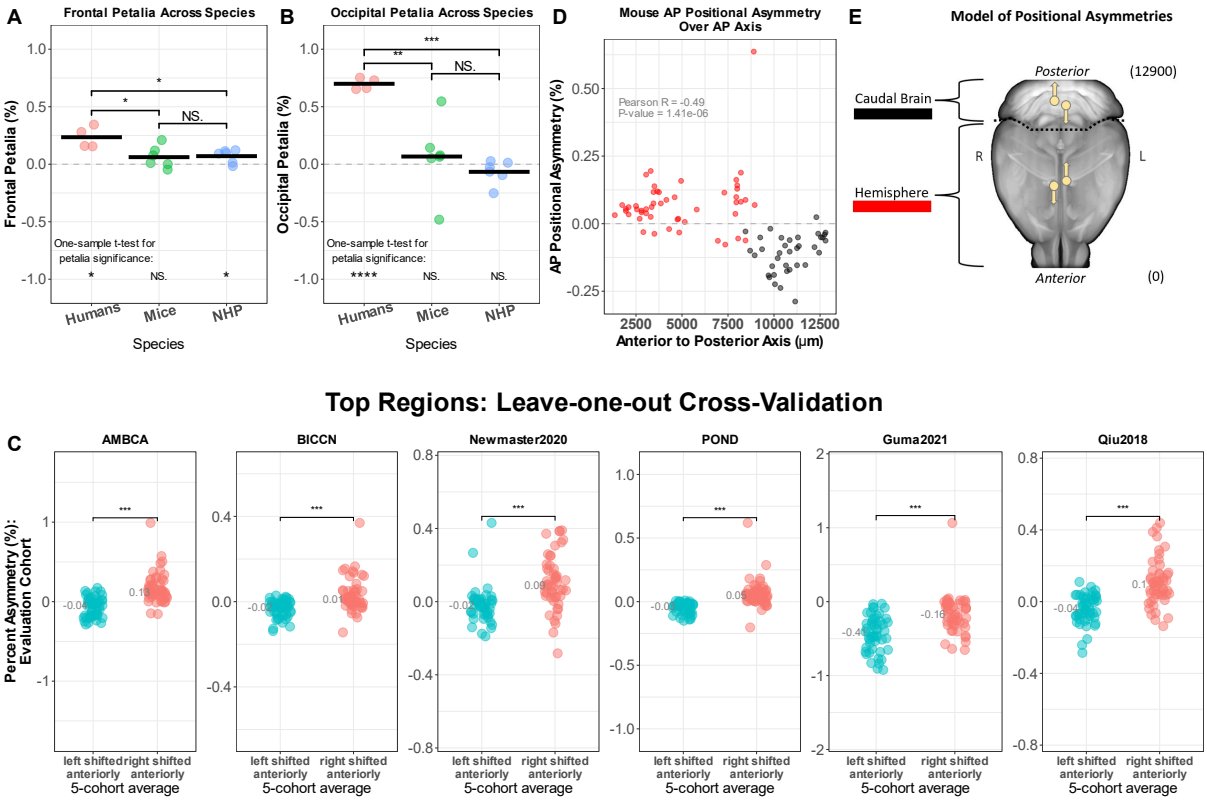

Figure 6. A-B) Cohort-specific petalia measurements for the **A)** frontal (anterior) or **B)** occipital (posterior) poles in humans (n = 4 cohorts, ~1400 individuals), mice (n = 6 cohorts, ~3500 individuals), or non-human primates (NHPs; n = 6 cohorts; 2 cohorts each for macaques, chimpanzees, and marmosets; ~1000 individuals). Each point on the graph is the average protrusion of subjects in that cohort, normalized against the length the left-hemisphere. A value of 0.2% means that the protrusion asymmetry is 0.2% the length of the left hemisphere on average. **C)** Leave-one-out cross-validation for the top positional asymmetries in all 6 cohorts. **D)** Anterior-posterior positional asymmetries derived from the mouse 6-cohort average, using the top 100 positional asymmetries. Regions that are shifted anteriorly on the right (positive values) tend to be found in the more anterior portions of the brain ("hemisphere"; red), while regions that are shifted anteriorly on the left (negative values) tend to be found in more posterior portions of the brain ("caudal brain"; black). Each point is a brain region and its color correspond to the definitions in E). **E)** Summary of positional asymmetries detected in C). "Caudal Brain" (black) is defined as midbrain, hindbrain, and cerebellum while everything anterior or dorsal to the midbrain is "hemisphere" (red). The "hemisphere" appears shifted anteriorly on the right while this trend appears opposite in the "caudal brain". *** is $p < 0.001$.

Figure 7. Cross-Species Comparisons of Volume Asymmetry

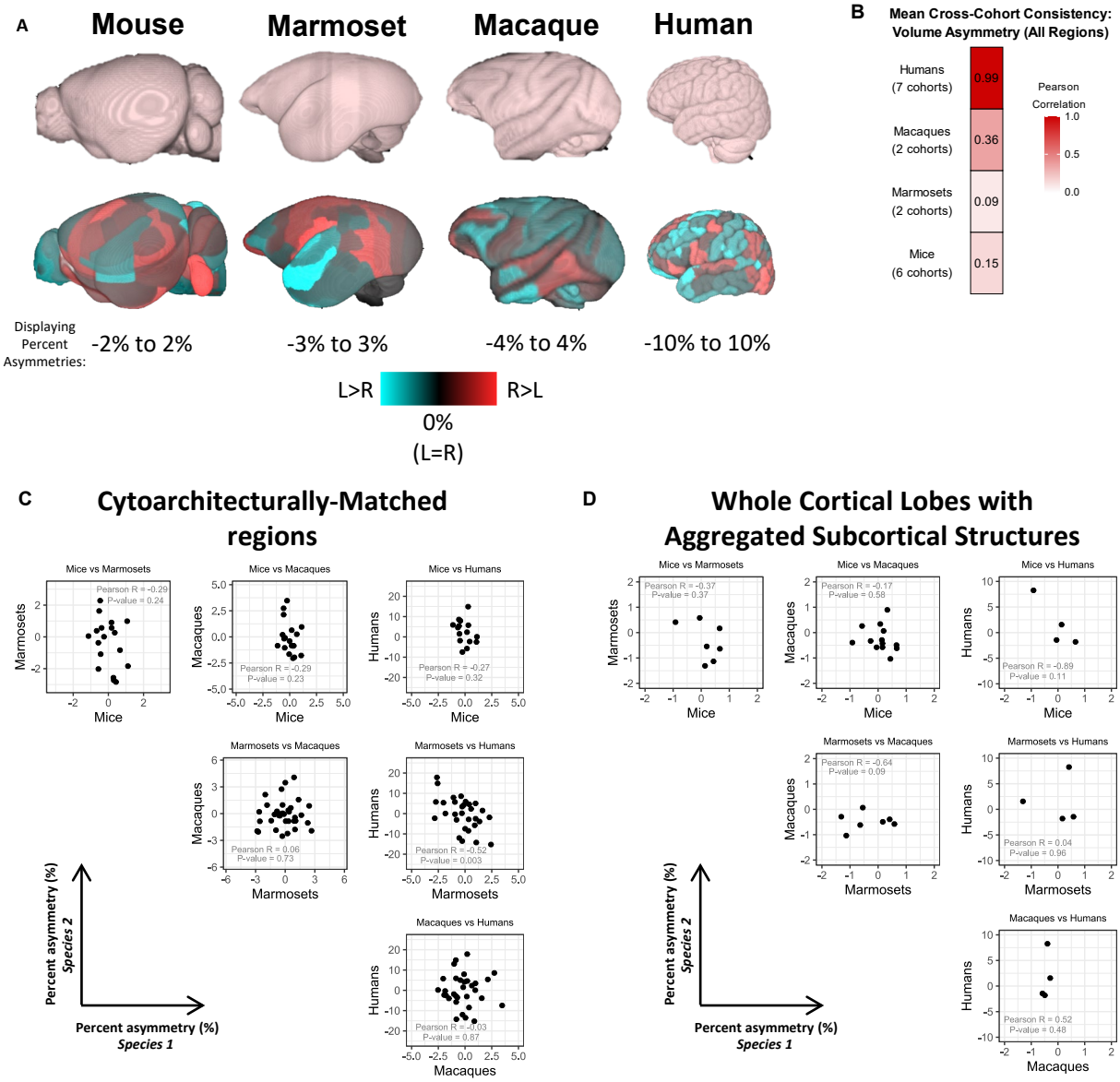

Figure 7. A) Top: 3D renderings of mouse, marmoset, macaque, and human brains from their respective 3D average templates. Middle: depiction of nominal volume asymmetry pattern for all regions in each atlas (regardless of significance), averaged across each cohort for that species. A minor brightness boost is added to better visualize the images. Bottom: display range of asymmetries shown for each species. **B)** The value in each cell and its color are the average cross-cohort consistency seen within a given species. Humans are the average of all 7 possible between-cohort combinations. Mice are similar but for 6 cohorts. Macaques and Marmosets have only 2 cohorts each, so the value indicates the lone Pearson correlation between the 2 cohorts in those species. **C-D)** Scatter plots of matched brain regions between species using the Garin et al. 2022 cross-species atlas. **C)** Cytoarchitecturally-matched (Brodmann) regions or **D)** summary values for whole cortical lobes and broad subcortical structures. Each species-pair has a different number of annotated regions which can be matched, hence the different number of data-points for each plot. Each point is a brain region. The value of the X- and Y-axes respectively indicate the cross-cohort average percent volume asymmetry observed in that species at that region. Human asymmetry data is only available for cortical regions.